ChemComm

Cite this: *Chem. Commun.*, 2012, **48**, 519–521

www.rsc.org/chemcomm

COMMUNICATION

Valine sulfonamidecinnamic acid asymmetric crystal reactions†

Kraig A. Wheeler,* Steven H. Malehorn and Annie E. Egan

Received 15th August 2011, Accepted 8th November 2011
DOI: 10.1039/c1cc15068e

Racemic and homochiral valine sulfonamidecinnamic acids crystallize with components aligned by use of the complementary features of hydrogen bonds and molecular topology to give supramolecular dimers. These discrete motifs effectively organize adjacent olefins for UV initiated single-crystal-to-single-crystal [2 + 2] photodimerization reactions. The racemic crystals produce inversion related cyclobutane products, while the desymmetrized crystalline architectures of the homochiral phase promote asymmetric photodimerization with 90% conversion.

Enhanced specificity and efficiency are hallmarks of chemical transformations that control molecular motion. Restricting the movement of components holds much importance to the development of functional materials such as catalysts[1] and molecular devices,[2] where the desired property frequently stems from a localized structural bias due to the combined effects of molecular shape and non-bonded contacts. While limiting motion can provide opportunities to differentiate reaction pathways or recognition profiles, high performance materials that result in complete or near quantitative selectivity require exquisite control of individual process components.

Though conceptually similar to the localized effects of solution processes, molecules aligned in crystalline architectures offer considerable advantage for enhanced spatial control. This benefit arises from building-blocks with fixed positions exhibiting long-range order. The intrinsic benefits of lattice-controlled molecules have long been realized with practical opportunities to produce new generation functional materials.[3] Utilizing crystalline architectures as *de novo* reaction vessels is one notable area that has attracted significant attention.

The unparalleled success of solid-state reactions over the last decade can partially be attributed to the identification and development of well-defined structural motifs.[4] Because motif prediction has evolved from exploration-based studies to more focused approaches utilizing a bottom-up design,[5] it is not surprising that reports of programmed reactivity from codified structural architectures are more commonplace in the literature. This collective work is largely directed at heteromeric assemblies, where at least one molecular component[5d–e] or metal center[5f–g] assists the alignment of neighboring reactive moieties. Progress realized in this field continues to offer much needed insight to the design and operational aspects of generating robust supramolecular synthons that exhibit solid-state reactivity. One remaining high-impact goal centers on successfully merging the structural predictability of these approaches with asymmetric reaction outcomes. Imprinting chirality on reaction processes provides a significant challenge that, if successful, promises considerable return to the scientific community in the form of new materials and applications. Essential outcomes now go beyond mild chemo- and stereoselective control and rest firmly with developing robust methods that result in high-yielding asymmetric syntheses. A recent review of this area illustrated several important examples that make use of unimolecular systems and enantiomorphic crystallization to control and preserve homochirality.[6] The principles of "crystal engineering" also emerged in this context; however, amplifying the predictability of these structural results to "total" asymmetric transformations remains a formidable challenge.[6,7]

Our recent attention to solid-state reactions developed an effective method for organizing chiral reactive components in the absence of secondary molecular/metal center templates.[8] As shown in Scheme 1, this strategy exploits sulfonamidecinnamic acid frameworks that form robust supramolecular dimers due to the features of molecular topology and directionality of hydrogen bonds. These dimeric motifs persist regardless of the use of racemic (*rac*)-**1**, quasiracemic [(*R*)-**1**/(*S*)-**2**], and homochiral single component (*R*)-**1** building-blocks. Each of these systems undergoes topochemically controlled[9] single-crystal-to-single-crystal (SCSC) photodimerization reactions in high yield (61–100% conversion). In the case of quasiracemate (*R*)-**1**/(*S*)-**2** and single component (*R*)-**1**, the homochiral molecules exert asymmetric induction on crystal growth and supramolecular dimer formation that ultimately translates to homochiral photodimer products. The current study presents several interesting opportunities to

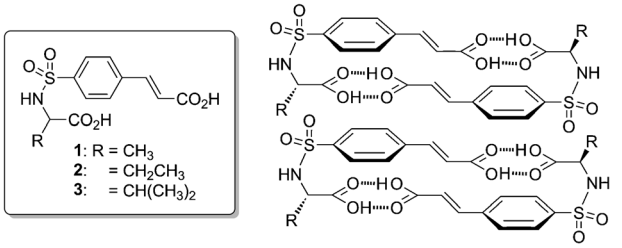

Scheme 1 Photoactive sulfonamidecinnamic acid frameworks (left) and supramolecular alignment of hydrogen-bonded dimers (right).

Department of Chemistry, Eastern Illinois University, Charleston Illinois, USA. E-mail: kawheeler@eiu.edu; Tel: 01 217 581 3119
† Electronic supplementary information (ESI) available: Synthetic procedures, photochemical details, and full crystal structure tables for (*rac*)- and (*R*)-**3**. CCDC 838809–838812. For ESI and crystallographic data in CIF or other electronic format see DOI: 10.1039/c1cc15068e

explore the supramolecular and photoreactive boundaries of this sulfonamidecinnamic acid framework. Use of racemic and homochiral valine **3** introduces an isopropyl group, spatially larger than Me and Et, into the structural framework that allows examination of the transferability of this approach and the role of the *R* group to crystal packing and solid-state photodimerization.

The target racemic and homochiral compounds of **3** were prepared using a straightforward two-step process.† Crystals of each phase were grown by slow evaporation of acetone solutions and assessed by X-ray crystallography.‡ In the case of (*rac*)-**3**, inspection of the crystal structure revealed components with the anticipated fishhook conformations organized into inversion related supramolecular dimers, topologically similar to those reported by Feldman *et al.*[10] (Fig. 1a). Each motif is stabilized by the complementary features of molecular shape and carboxyl···carboxyl hydrogen bonds that effectively aligns adjacent olefins with <3.8 Å separation. The discrete pattern present in (*rac*)-**3** is nearly indistinguishable to those reported for the alanine and butyrate phases[8a] [*i.e.* (*rac*)-**1**, (*R*)-**1**/(*S*)-**2**] and, thus highlights the strong preference of sulfonamidecinnamic acids to form supramolecular dimers.

The pendant isopropyl group of racemic **3** provides a critical departure from the crystal packing motifs generated by compounds **1** and **2**. As shown in Fig. 1 (right), assessment of these previous structures revealed hydrogen-bonded dimers with favorable olefin···olefin alignment for both the intra- and interdimer motifs. Though the X-ray data suggested [2 + 2] cycloaddition preferentially occurred by the intradimer path, products generated *via* an interdimer process could not be initially discounted. In view of this potential structural dilemma, how to effectively isolate these hydrogen-bonded dimers in the solid-state raises an important challenge. Compound (*rac*)-**3** effectively circumvents this issue by use of the spatial properties of the pendant isopropyl group; where the steric bulk of this group disrupts the close alignment of interdimer olefins and displaces adjacent dimers with a slip distance of $\sim$3.0 Å. Because the C=C groups of these next nearest neighbors are separated by 4.5 Å, the increased size of *R* supplies an effective structural handle to isolate the hydrogen bonded motifs and, in turn, the photodimerization process.

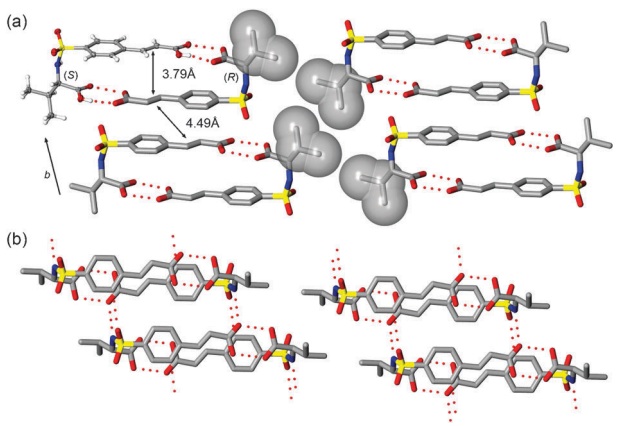

Fig. 1 Two views of the crystal structure of (*rac*)-**3** showing the (a) asymmetric unit (50% probability) and packing motif and (b) formation of extended hydrogen-bond motifs.

A single crystal of (*rac*)-**3** was illuminated using a 200W Xe(Hg) lamp and the long wavelength tail-irradiation technique.[11]† Because no appreciable crystal degradation was observed, reaction progress was periodically monitored by collecting full sets of X-ray data.‡ Refinement of the occupancy factors for the reactant and product phases provided a straightforward method for analysing this SCSC transformation. This photodimerization process proceeded in 68% conversion after 7.2 h of exposure (Fig. 2).

Though our original program design of sulfonamidecinnamic acids focused on exploiting the inversion symmetry (or near inversion symmetry) preferences[12] of organic racemates and quasiracemates, early success with these materials prompted further study of more diverse chemical systems. At first we reasoned that chiral single-component compounds, *e.g.* (*R*)-**1**, seemed unlikely candidates given such materials, when recrystallized, form desymmetrized motifs lacking the desired inversion symmetry requirement. To our surprise, slow evaporation crystal growth of (*R*)-**1** from acetone and 2-butanone resulted in three polymorphic forms; each displaying approximate centrosymmetric supramolecular dimers.[8b] In addition to (*rac*)-**3**, this paper also examines the structure of homochiral valine (*R*)-**3** that further strengthens the importance of the central sulfonamidecinnamic acid framework to hydrogen-bond dimer construction. (*R*)-**3** crystallized in space group *P*1 with two symmetry independent molecules ($Z' = 2$). Fig. 3 shows these molecular pairs assemble into homomeric dimers with short 3.81 Å olefinic spacing. While rigorously chiral, these motifs exhibit a remarkable degree of centrosymmetry as indicated by a low S(*Ci*) value (0.14) determined using Avnir's Continuous Symmetry Method.[13] The alignment of dimers in the crystal follows a similar pattern observed for racemate **3**, where the increased spatial properties of the isopropyl group in (*R*)-**3** divert the structure from close-packed infinite stacks of olefins to isolated dimers.

Photodimerization of a single crystal of (*R*)-**3** *via* tail-irradiation resulted in asymmetric synthesis of the cyclobutane product. Reaction progress was again scrutinized by X-ray crystallography (Fig. 4, top). At 15% conversion (20 min), crystal quality greatly diminished as evident from visual inspection of the sample (crystal fractures and discoloration) and diffuse, less-intense reflections in the X-ray diffraction pattern. A powder sample of (*R*)-**3** was then treated with unfiltered UV radiation and periodically assessed by ^{1}H NMR. As shown in Fig. 4 (bottom), the distinct NMR signals of the olefin (6.7 and 7.7 ppm) and cyclobutane (4.1 and 4.5 ppm) protons allow evaluation of the reaction progress.

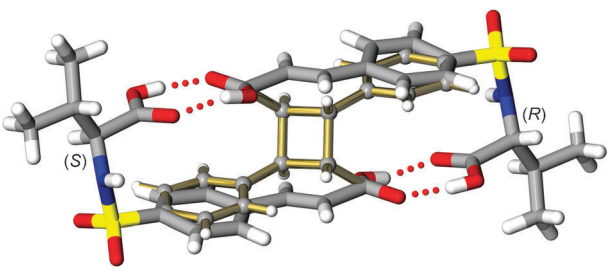

Fig. 2 Crystal structure of UV-irradiated (*rac*)-**3** indicating reactant and cyclobutane product phases (32 : 68, 7.2 h).

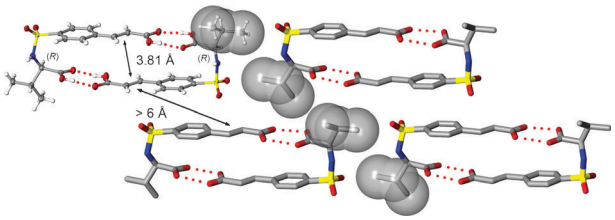

Fig. 3 Structure of (*R*)-**3** showing the asymmetric unit (50% probability) and spatial influence of the isopropyl group.

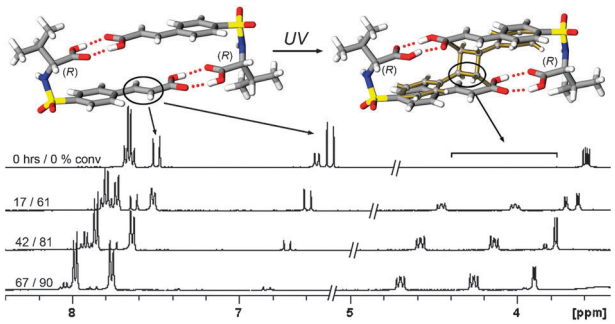

Fig. 4 Solid-state photodimerization of (*R*)-**3** assessed using single-crystal X-ray diffraction (top) and ^{1}H NMR (bottom).

Such experimental results indicate a time dependent decrease in reactant and increase in product signals with 90% conversion (67 h).

In summary, the persistent formation of supramolecular dimers underscores this approach as a viable method for organizing programmed reactivity in molecular crystals. Despite the chemical and spatial diversity of alkyl groups inspected to date (*i.e.* Me, Et, and *i*-Pr), the recognition profiles of these sulfonamidecinnamic acids result in fish hook conformations and discrete motifs that efficiently direct [2 + 2] photocylcoaddition reactions. Both (*rac*)-**3** and (*R*)-**3** undergo remarkable SCSC transformations that result in achiral and homochiral photoproducts, respectively.

This work was supported by the National Science Foundation (CHE-0957391 and CHE-0722547).

Notes and references

‡ *Crystallographic data*. X-ray diffraction data for (*rac*)- and (*R*)-**3** were collected with a Bruker APEX-II equipped with a graphite-monochromator using Cu-Kα radiation (λ = 1.54178 Å).

Crystal data for (*rac*)-**3** (reactant): $C_{14}H_{17}NO_6S$, M_r = 327.35, Triclinic space group $P\bar{1}$, a = 7.2401(1), 7.2996(1), c = 15.8742(3) Å, α = 88.734(1), β = 87.853(1), γ = 64.951(1)°, V = 759.49(2) Å^3, Z = 2, D_c = 1.431 g cm^{-3}, μ = 2.169 mm^{-1}, F_{000} = 344, T = 100(2)K, $2\theta_{max}$ = 68.24°, 15 072 reflections collected (2710 unique), R_1 = 0.0485 and wR_2 = 0.1270 [$I > 2\sigma(I)$], R_{int} = 0.0467, GOF = 1.12.

Crystal data for (*rac*)-**3** (photodimerized): $C_{28}H_{34}N_2O_{12}S_2$, M_r = 654.71, Triclinic space group $P1$, a = 7.4391(3), b = 7.6719(3), c = 15.0529(7) Å, α = 88.371(3), β = 85.421(3), γ = 61.552(2)°, V = 752.91(5) Å^3, Z = 1, D_c = 1.444 g cm^{-3}, μ = 2.188 mm^{-1}, F_{000} = 344, T = 100(2)K, $2\theta_{max}$ = 66.77°, 13 224 reflections collected (2563 unique), R_1 = 0.0751 and wR_2 = 0.1959 [$I > 2\sigma(I)$], R_{int} = 0.0623, GOF = 1.15.

Crystal data for (*R*)-**3** (reactant): $C_{14}H_{17}NO_{16}S$, M_r = 327.35, Triclinic space group $P1$, a = 7.9008(2), b = 8.0121(2), c = 11.8061(3) Å, α = 83.617(1), β = 77.774(2), γ = 88.744(2)°, V = 725.87(3) Å^3, Z = 2, D_c = 1.498 g cm^{-3}, μ = 2.269 mm^{-1}, F_{000} = 344, T = 100(2)K, $2\theta_{max}$ = 67.57°, 4857 reflections collected (4857 unique, two-component twin), R_1 = 0.0423 and wR_2 = 0.1077 [$I > 2\sigma(I)$], R_{int} = 0.0461, GOF = 1.08, *flack* = 0.54(6).

Crystal data for (*R*)-**3** (photodimerized): $C_{28}H_{34}N_2O_{12}S_2$, M_r = 654.71, Triclinic space group $P1$, a = 7.8647(3), b = 8.0522(3), c = 11.7930(5) Å, α = 83.951(2), β = 77.725(2), γ = 89.754(2)°, V = 725.57(5) Å^3, Z = 1, D_c = 1.498 g cm^{-3}, μ = 2.270 mm^{-1}, F_{000} = 344, T = 100(2)K, $2\theta_{max}$ = 67.32°, 4698 reflections collected (4698 unique, two-component twin), R_1 = 0.0499 and wR_2 = 0.1250 [$I > 2\sigma(I)$], R_{int} = 0.0581, GOF = 1.03, *flack* = 0.09(2).

1 For selected reviews, see: J. F. Hartwig, *Organotransition Metal Chemistry: From Bonding to Catalysis*, University Science Books, Mill Valley, CA, 2010; *Polymeric Chiral Catalyst Design and Chiral Polymer Synthesis*, ed. S. Itsuno, Wiley-VCH Verlag GmbH, Weinheim, Germany, 2011; X. Sun, C. J. Reedy and B. R. Gibney, *Chem. Rev.*, 2004, **104**, 617; *Organocatalysis*, ed. M. T. Reetz, B. List, S. Jaroch and H. Weinmann, Springer, Berlin, 2008; H. U. Vora and T. Rovis, *Aldrichimica Acta*, 2011, **44**, 3.

2 For selected reviews, see: *Molecular Devices and Machines*, ed. V. Balzani, A. Credi and M. Venturi, Wiley-VCH Verlag GmbH, Weinheim, Germany, 2008; V. Balzani, A. Credi and M. Venturi, *Chem. Soc. Rev.*, 2011, **38**, 1542; Y. Krishnan and F. C. Simmel, *Angew. Chem., Int. Ed.*, 2011, **50**, 3124; E. M. Pérez, *Angew. Chem., Int. Ed.*, 2011, **50**, 3359.

3 Y. Liu, C. Hu, A. Comotti and M. D. Ward, *Science*, 2011, **333**, 436; S. D. Karlen, H. Reyes, R. E. Taylor, S. I. Khan, M. F. Hawthorne and M. A. Garcia-Garibay, *Proc. Natl. Acad. Sci. U. S. A.*, 2010, **107**, 14973.

4 *Organic Crystal Engineering: Frontiers in Crystal Engineering*, ed. E. R. T Tiekink, J. Vittal and M. Zaworotko, John Wiley & Sons, Ltd, Chichester, UK, 2010; G. R. Desiraju, *Angew. Chem., Int. Ed.*, 2007, **46**, 8342; C. B. Aakeröy, N. R. Champness and C. Janiak, *CrystEngComm*, 2010, **12**, 22.

5 (*a*) M. B. Hickey, R. F. Schlam, C. Guo, H. Chengyun, T. H. Cho, B. B. Snider and B. M. Foxman, *CrystEngComm*, 2011, **13**, 3146; (*b*) I. Zouev, D.-K. Cao, T. V. Sreevidya, M. Telzhensky, M. Botoshansky and M. Kaftory, *CrystEngComm*, 2011, **13**, 4376; (*c*) D.-K. Cao, T. V. Sreevidya, M. Botoshansky, G. Golden, J. Benedict and M. Kaftory, *J. Phys. Chem. A*, 2010, **114**, 7377; (*d*) R. Santra and K. Biradha, *CrystEngComm*, 2011, **13**, 3246; L. R. MacGillivray, *J. Org. Chem.*, 2008, **73**, 3311; (*e*) G. K. Kole, G. K. Tan and J. J. Vittal, *Org. Lett.*, 2010, **12**, 128; (*f*) D. Liu, Z.-G. Ren, H.-X. Li, J.-P. Lang, N.-Y. Li and B. Abrahams, *Angew. Chem. Int. Ed.*, 2010, **49**, 4767; (*g*) M. Nagarathinam, A. M. P. Peedikakkal and J. J. Vittal, *Chem. Commun.*, 2008, 5277.

6 I. Weissbuch and M. Lahav, *Chem. Rev.*, 2011, 3236.

7 M. Vaida, L. J. W. Shimon, J. van Mil, K. Ernst-Cabrera, L. Addadi, L. Leiserowitz and L. Lahav, *J. Am. Chem. Soc.*, 1989, **111**, 1029; M. Vaida, L. J. W. Himon, Y. Weisinger-Lewin, F. Frolow, H. Lahav, L. Leiserowotz and R. K. McMullan, *Science*, 1988, **241**, 1475; F. Toda and K. Mori, *J. Chem. Soc., Chem. Commun.*, 1989, **17**, 1245; F. Toda, in *Topics in Stereochemistry Vol. 25*, ed. S. E. Denmark and J. S. Siegel, John Wiley & Sons, Hoboken, NJ, 2006, ch. 1, pp. 1–29.

8 (*a*) R. C. Grove, S. H. Malehorn, M. E. Breen and K. A. Wheeler, *Chem. Commun.*, 2010, **46**, 7322; (*b*) K. A. Wheeler, J. D. Wiseman and R. C. Grove, *CrystEngComm*, 2011, **13**, 3134.

9 M. D. Cohen and G. M. J. Schmidt, *J. Chem. Soc.*, 1964, 1996.

10 K. S. Feldman, R. F. Campbell, J. C. Saunders, C. Ahn and K. M. Masters, *J. Org. Chem.*, 1997, **62**, 8814.

11 M. Kahn, V. Enkelmann and G. Brunklaus, *Cryst. Growth Des.*, 2009, **9**, 2354; I. Abdelmoty, V. Buchholz, L. Di, V. Enkelmann, G. Wegner and B. M. Foxman, *Cryst. Growth Des.*, 2005, **5**, 2210; J. B. Benedict and P. Coppens, *J. Phys. Chem. A*, 2009, **113**, 3116.

12 S. P. Kelley, L. Fabian and C. P. Brock, *Acta. Crystallogr.*, 2011, **B67**, 79; M. Hendi, P. Hooter, V. Lynch, R. E. Davis and K. A. Wheeler, *Cryst. Growth Des.*, 2004, **4**, 95; B. Dalhus and C. H. Gorbitz, *Acta Crystallogr., Sect. B: Struct. Sci.*, 2000, **B56**, 715.

13 C. Dryzun, A. Zait and D. Avnir, *J. Comput. Chem.*, 2011, **32**, 2526.